Available online at www.sciencedirect.com
ScienceDirect
Physica E 37 (2007) 163–167
PHYSICA E
www.elsevier.com/locate/physe

Characteristics of SiO_x nanowires synthesized via the thermal heating of Cu-coated Si substrates

Hyoun Woo Kim*, Seung Hyun Shim, Jong Woo Lee

School of Materials Science and Engineering, Inha University, Incheon 402-751, Republic of Korea

Available online 13 October 2006

Abstract

We have demonstrated the growth of SiO_x nanowires by the simple heating of the Cu-coated Si substrates. We have applied X-ray diffraction, scanning electron microscopy and transmission electron microscopy techniques to characterize the structure of the samples. The as-synthesized SiO_x nanowires had amorphous structures with diameters in the range of 20–80 nm. The thickness of the Cu layer affected the resultant sample morphology, favoring the nanowire formation at smaller thickness. Photoluminescence spectra of the nanowires exhibited blue emission. We have proposed the possible growth mechanism.

PACS: 61.46.+w; 78.55.−m; 81.07.−b

Keywords: Nanostructures; Chemical synthesis; Transmission electron microscopy

1. Introduction

Since one-dimensional (1D) nanomaterials in the form of tubes, wires, and belts have attracted much attention because of their interesting geometries, novel properties, and potential applications [1–3], considerable efforts have been placed on the synthesis and characterization of those materials over the past several years.

Silicon (Si) and silica (SiO_x) nanostructures have attracted considerable attention due to their unique properties and promising application in mesoscopic research, nanodevices, and opto-electronics devices [4–6]. Particularly, SiO_x is an important material for photoluminescence (PL) [7,8]. Since the majority of SiO_x nanowires fabrication methods are catalyst-based methods, different kinds of metal catalysts have been used, such as Au [9–13], Pd–Au [14], Fe [15–18], Ga [19,20], Ga–In [21], Ni [22], In–Ni [23], Sn [24], and Co [25].

Copper (Cu) is a good conductor of heat and electricity (secondly only to silver in electrical conductivity) and has long been widely used in electronic devices. However, to our best knowledge, synthesis of any inorganic nanostructure on Cu substrates has not been reported to date.

In this paper, for the first time we report the production of SiO_x nanowires by the simple heating of Cu-coated Si substrates. We have investigated the effect of Cu layer thickness on the growth of SiO_x nanowires. We discuss the possible growth mechanism with respect to the role of the predeposited Cu layers.

2. Experimental

The growth process was carried out in a quartz tube. The experimental apparatus has been described elsewhere [26]. We have employed Cu-coated Si substrates. In order to fabricate the Cu-coated Si substrates, we used Si as starting materials onto which a layer of Cu in the range 15–60 nm was deposited by the sputtering.

On top of the alumina boat, a piece of the substrate was placed with the Cu-coated side downwards. The quartz tube was inserted into a horizontal tube furnace. During the experiment, a constant pressure with an air flow (~3.1% O_2 in a balance of argon) was maintained at 300 mTorr. The furnace was heated at a rate of 10 °C min^{-1} to a target temperature of 1000 °C. After 2 h of typical

*Corresponding author. Tel.: +82 32 860 7544; fax: +82 32 862 5546.
E-mail address: hwkim@inha.ac.kr (H.W. Kim).

1386-9477/$ - see front matter © 2006 Elsevier B.V. All rights reserved.
doi:10.1016/j.physe.2006.09.001

deposition process at 1000 °C, the substrate was cooled down and then removed from the furnace for analysis.

As-grown samples were investigated and analyzed using glancing angle (0.5°) X-ray diffraction (XRD, X'pert MPD-Philips with CuKα_1 radiation), scanning electron microscopy (SEM, Hitachi S-4200), and transmission electron microscopy (TEM, Philips CM-200) with energy-dispersive X-ray (EDX) spectroscopy attached. TEM samples were prepared by sonicating the substrate in acetone by ultrasonic treatment. A drop of the dispersion solution was then placed on a porous carbon film supported on a gold grid. PL spectra of the samples were measured in a SPEX-1403 photoluminescence spectrometer with a He–Cd laser (325 nm, 55 mW) at room temperature.

3. Results and discussion

Fig. 1a shows the SEM top views of the sample morphology on the Cu-coated Si substrates, in which the thickness of the predeposited Cu layer was about 15 nm. There are randomly oriented nanowires on the substrate. Statistical observation of many SEM images indicated that the diameter of nanowires varied from 20 to 80 nm. Fig. 1b shows the cross-sectional SEM image, indicating that the tangled nanowires are grown on the substrate. It is noteworthy that there is a highly undulated interface between the nanowire layer and the substrate, suggesting that the nanowires are rooted from the substrate. Fig. 1c shows the XRD patterns of the product, revealing that the nanowires are fully amorphous. No reflections are clearly discerned other than the (2 0 0) diffraction peak of Cu (JCPDS: 04-0836), possibly from the substrate.

TEM shows the general morphology and dimension of SiO_x nanowires. Figs. 2a and b show the TEM images of the product, indicating that this raw material indeed consists of aggregates of nanowires. Although most nanowires have straight or smoothly curved morphology, some nanowires indicated by arrow 1 exhibit the helical structure (Fig. 2a). The similar helical nanowires were previously produced by using the Fe catalysts [16,18]. In addition, nanoparticles (indicated by arrow 2 in Fig. 2b) were observed in the middle and/or at the ends of the wires. As shown in the inset of Fig. 2a, the highly dispersed selected area electron diffraction (SAED) pattern indicates that the nanowires are amorphous. Fig. 2c shows a HRTEM image of a single nanowire, indicating that the nanoparticle at the tip of the nanowire appears dark and have high contrast compared with the nanowire stem. A thin amorphous layer of 3–8 nm thickness exists on the surface of nanoparticle at the tip.

EDX measurement made on the wire stem reveals that the nanowire stem consists of Si and O (Fig. 2d). Au signals are generated from the gold grid on which these nanowires were supported. EDX spectrum on the wire tip shows the signals of Si, O, Au, and Cu elements (Fig. 2e). By comparing Fig. 2e with d, although we do not know the exact chemical composition of the nanoparticle, we

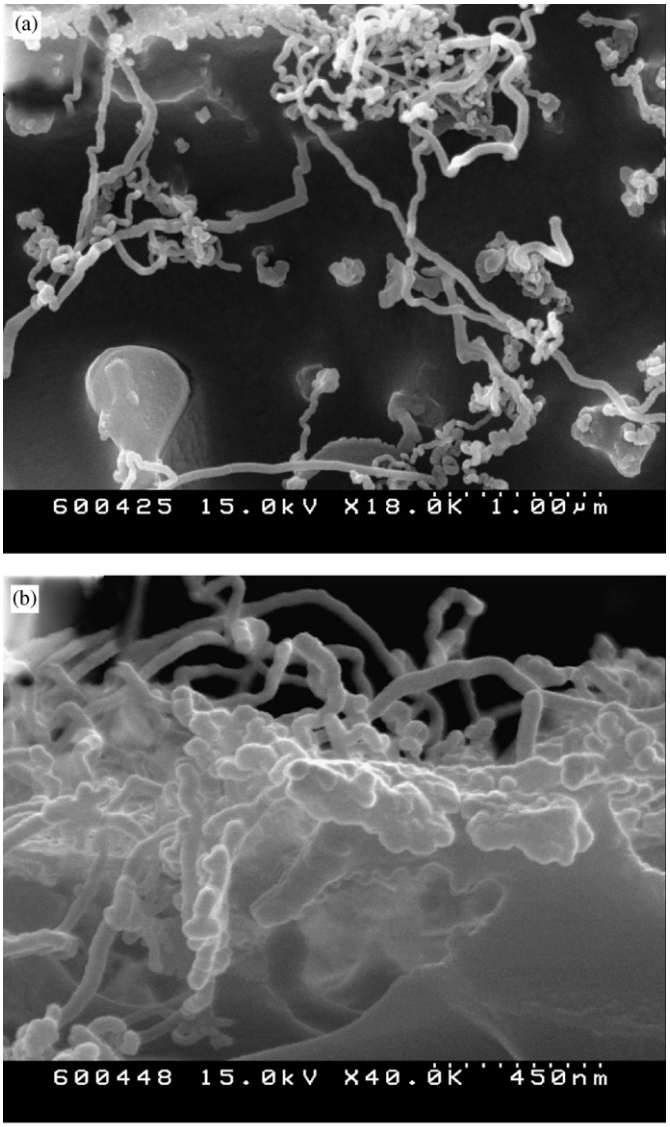

Fig. 1. (a) Plan-view; (b) side-view SEM images of the product and (c) X-ray diffraction pattern recorded from the product.

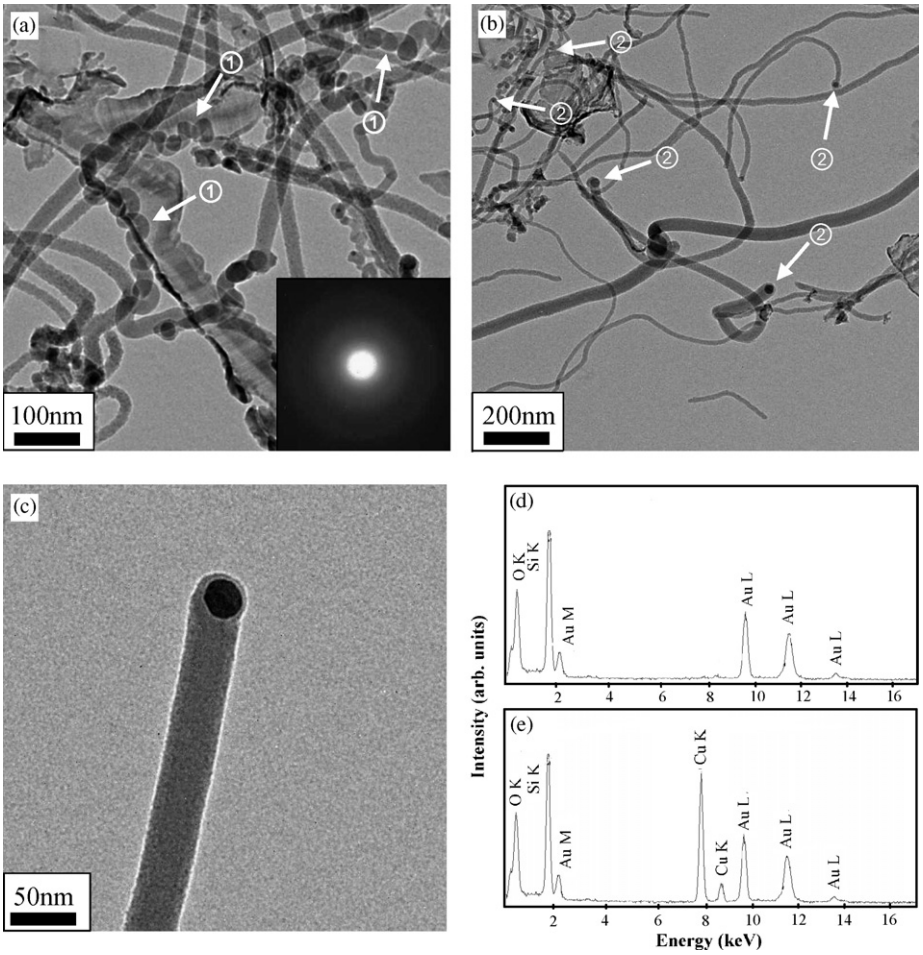

Fig. 2. (a,b) Low-magnification TEM images showing the general morphology of SiO_x nanowires (Arrow 1: helical nanowires or nanosprings; Arrow 2: nanoparticles). The lower right inset of (a) is the SAED pattern of SiO_x nanowires. (c) HRTEM image of a single nanowire. The nanowire terminates with a nanoparticle. EDX spectra of (d) the wire stem and (e) the wire tip.

propose that the nanoparticle at least comprises a Cu element.

The solidified spherical droplet at the tip or in the middle of the nanowires is commonly considered to be the evidence for the operation of the vapor–liquid–solid (VLS) mechanism, which is in agreement with our experimental conditions and the observed results. Since the available Si source was the substrate itself, it is interesting to note that the present synthetic process mainly involves the solid phase with respect to the Si elements. Similarly, various forms of SiO_x nanowires including straight, curved, and helical-shaped nanowires have been fabricated previously using the VLS method [10,13–16, 19–21,23,24].

The growth of the SiO_x nanowires in the present study can be divided into several steps. In the first step, when the Si wafer with Cu film was heated, the Cu/Si liquid droplets will form at 1000 °C because of its relatively low eutectic temperature (802 °C) [27]. In the second step, the droplets or nanoparticles act as the nucleation sites, initiating the growth of SiO_x nanowires. The liquid state particles should easily absorb oxygen and the presence of a relatively small amount of oxygen is not expected to change the Cu–Si phase diagram significantly. The most likely source of oxygen may come from the O_2 in the carrier gas, while the oxygen adsorbed on the Si wafer due to air exposure during the processing and the residual oxygen in the tube can be other sources. No extra Si source other than Si substrate was introduced in the present study. The undulated interface as shown in Fig. 1b also supports that Si originated from the substrate. As the droplets become supersaturated, amorphous SiO_x nanowires are formed, possibly by the reaction between Si and O. In the third step, by continuously dissolving Si and O onto nanoparticles, the SiO_x nanowires may subsequently grow. The droplet will continuously absorb Si atoms as it is abundant in the system. Also, the O_2 in the carrier gas can supply a constant oxygen source during the process.

In order to investigate the role of Cu layer thickness played in the formation of SiO_x nanowires, we have varied the film thickness in the range of 15–60 nm. As shown in Fig. 3, different Cu layer thicknesses gave different results. We have obtained the bundles of nanowires at 15 nm, whereas we only observe the big islands by using a 60 nm-thick Cu layer. With the thick layer of 30 nm, few nanowires start to form as shown in Fig. 3b. To

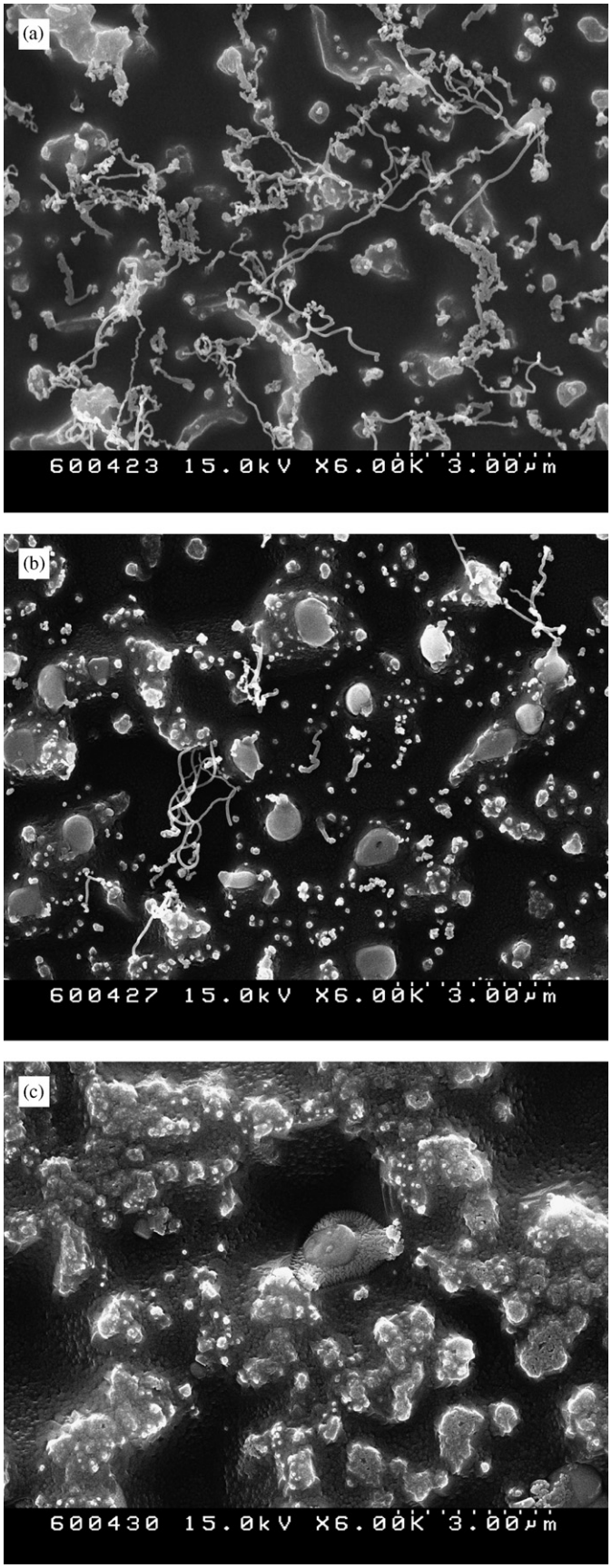

Fig. 3. Plan-view SEM images of the product with the Cu layer thicknesses of: (a) 15 nm; (b) 30 nm, and (c) 60 nm.

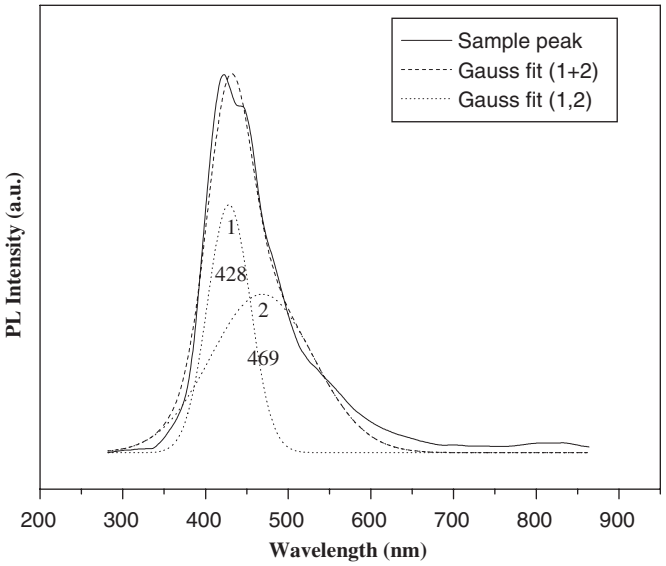

Fig. 4. PL of the SiO_x nanowires. The blue light emission was revealed peaking at 421 and 448 nm.

summarize, we observed that the areal density of the SiO_x nanowires decreased with increasing the Cu layer thickness. When the Cu layer is relatively thin, the 1000 °C-heating during the synthesis process presumably promotes the agglomeration of Cu layer and thus the formation of the island-like structures with a wide interspace. Therefore, nanowires may be formed independently from the locally present small islands. On the other hand, the relatively thick Cu layer may not be transformed into the small enough islands. The formed big islands may provide dense nucleation sites, generating the cluster-like structures by the interference and agglomeration of SiO_x nuclei. Although we have succeeded in providing a route to fabricating the 1D materials of SiO_x, further experimental study is needed to fine-tune the growth process and to clearly understand the synthesis mechanism.

Fig. 4 shows the PL spectrum of the SiO_x nanowires measured at room temperature, which is an apparent broad emission band mainly located in the visible region. Gaussian fitting analysis showed that the broad emission band was a superimposition of two major peaks at 428 and 469 nm, respectively. The similar blue emission with a peak position in the range of 414–470 nm have been previously observed in the PL spectrum of SiO_x nanowires [11,13,15,28], which was ascribed to neutral oxygen vacancy or oxygen deficiency-related diamagnetic defect centers [15]. We believe that the blue light emission from the SiO_x nanowires in the present study can be attributed to the above-mentioned defects arising from oxygen deficiency, presumably being generated during the high temperature synthetic process.

4. Conclusion

In summary, we have achieved the growth of SiO_x nanowires through a Cu-catalyzed process. SEM images

indicate that the nanowires have diameters in the range of 20–80 nm. XRD, SAED, and EDX analyses reveal that the nanowires are amorphous and consist only of silicon oxide. The growth of SiO_x nanowires is most likely controlled by the VLS mechanism with Cu-related catalytic particles. By varying the thickness of Cu layer, we reveal that thin enough Cu layer promotes the production of nanowires. The room-temperature PL measurement with the Gaussian fitting shows apparent blue light emission bands centered at 428 and 469 nm.

Acknowledgment

This work was supported by Inha Research Fund 2006.

References

[1] S. Iijima, Nature 354 (1991) 56.
[2] A. Morales, C.M. Lieber, Science 279 (1998) 208.
[3] Z.W. Pan, Z.R. Dai, Z.L. Wang, Science 291 (2001) 1947.
[4] S. Mann, G.A. Ozin, Nature 382 (1996) 313.
[5] A. Katz, M.E. Davis, Nature 403 (2000) 286.
[6] C.T. Kresge, M.W. Leonowicz, W.J. Roth, J.C. Vartuli, J.S. Beck, Nature 359 (1999) 710.
[7] H. Nishikawa, T. Shiroyama, R. Nakamura, Y. Ohiki, K. Nagasawa, Y. Hama, Phys. Rev. B 45 (1992) 586.
[8] L.S. Liao, X.M. Bao, X.Q. Zhang, N.S. Li, N.B. Min, Appl. Phys. Lett. 68 (1996) 850.
[9] S.-H. Li, X.-F. Zhu, Y.-P. Zhao, J. Phys.Chem. B 108 (2004) 17032.
[10] J.S. Wu, S. Dhara, C.T. Wu, K.H. Chen, Y.F. Chen, L.C. Chen, Adv. Mater. 14 (2002) 1847.
[11] Z.Q. Liu, S.S. Xie, L.F. Sun, D.S. Tang, W.Y. Zhou, C.Y. Wang, W. Liu, Y.B. Li, X.P. Zou, G. Wang, J. Mater. Res. 16 (2001) 683.
[12] M. Paulose, O.K. Varghese, C.A. Grimes, J. Nanosci. Nanotechnol. 3 (2003) 341.
[13] Y.W. Wang, C.H. Liang, G.W. Meng, X.S. Peng, L.D. Zhang, J. Mater. Chem. 12 (2002) 651.
[14] J.L. Elechiguerra, A. Camacho-Bragado, J. Manriquez, J.P. Zhou, M. Jose-Yacaman, Microsci. Microanal. 10 (2004) 388.
[15] D.P. Yu, Q.L. Hang, Y. Ding, H.Z. Zhang, Z.G. Bai, J.J. Wang, Y.H. Zou, W. Qian, G.C. Xiong, S.Q. Feng, Appl. Phys. Lett. 73 (1998) 3076.
[16] H.-F. Zhang, C.-M. Wang, E.C. Buck, L.-S. Wang, Nano Lett. 3 (2003) 577.
[17] X.C. Wu, W.H. Song, K.Y. Wang, T. Hu, B. Zhao, Y.P. Sun, J.J. Du, Chem. Phys. Lett. 336 (2001) 53.
[18] C.H. Liang, L.D. Zhang, G.W. Meng, Y.W. Wang, Z.Q. Chu, J. Non-cryst. Solids 277 (2000) 63.
[19] Z. Pan, S. Dai, D.B. Beach, D.H. Lowndes, Nano Lett. 3 (2003) 1279.
[20] Z.W. Pan, Z.R. Dai, C. Ma, Z.L. Wang, J. Am. Chem. Soc. 124 (2002) 1817.
[21] J.C. Wang, C.Z. Zhan, F.G. Li, Solid State Commun. 125 (2003) 629.
[22] Z. Zhang, G. Ramanath, P.M. Ajayan, D. Golberg, Y. Bando, Adv. Mater. 13 (2001) 197.
[23] R. Ma, Y. Bando, Chem. Phys. Lett. 377 (2003) 177.
[24] S.H. Sun, G.W. Meng, M.G. Zhang, Y.T. Tian, T. Xie, L.D. Zhang, Solid State Commun. 128 (2003) 287.
[25] H. Takikawa, M. Yatsuki, T. Sakakibara, Jpn. J. Appl. Phys. 38 (1999) L401.
[26] H.W. Kim, N.H. Kim, J.H. Myung, S.H. Shim, Phys. Stat. Sol. (A) 202 (2005) 1758.
[27] T.B. Massalski, first ed, Binary alloy phase diagrams, Vol. 1, American Society for Metals, Metals Park, Ohio, 1986, p. 960.
[28] G.Z. Ran, L.P. You, L. Dai, Y.L. Liu, Y. Lv, X.S. Chen, G.G. Qin, Chem. Phys. Lett. 384 (2004) 94.